SCIENCE CHINA
Chemistry

• ARTICLES •

December 2010 Vol.53 No.12: 2637–2643
doi: 10.1007/s11426-010-4160-3

Heterogeneous reaction of SO_2 on TiO_2 particles

SHANG Jing*, LI Jia & ZHU Tong*

State Key Joint Laboratory of Environmental Simulation and Pollution Control;
College of Environmental Sciences and Engineering, Peking University, Beijing 100871, China

Received July 2, 2010; accepted September 24, 2010

The heterogeneous reaction of SO_2 on TiO_2 particles was studied using *in situ* diffuse reflectance infrared Fourier transform spectroscopy (DRIFTS). The influences of the oxygen concentration, relative humidity (RH), and ultraviolet (UV) light illumination ($\lambda \approx 365$ nm) intensity on the reaction were investigated. The main product of the heterogeneous reaction of SO_2 on TiO_2 particles was sulfate with UV illumination and sulfite without it. The production of sulfate was promoted significantly with UV illumination or water, and there was a synergistic effect when both were present. In the dry system without UV, the heterogeneous reaction of SO_2 on TiO_2 particles was found to be second-order for SO_2 and the initial uptake coefficient, γ_{BET}, was determined to be 1.94×10^{-6}. With UV and RH = 40%, the reaction order was first-order and the initial uptake coefficient was 1.35×10^{-5}.

SO_2, TiO_2, DRIFTS, heterogeneous oxidation

1 Introduction

Sulfur dioxide (SO_2) is one of the major gaseous pollutants in the atmosphere, where it is an important precursor of acid rain. It can be oxidized into sulfuric acid or sulfate by O_3, ·OH, and other radicals. Acid rain can damage entire ecosystems and sulfate aerosols influence global climate change via direct and indirect irradiative forcing [1–3]. The inhalation of SO_2 can induce or cause deterioration of respiratory diseases, such as asthma [4]. The main source of SO_2 in the atmosphere is emissions from the burning of sulfur-containing fossil fuels. Thus, the distribution of SO_2 shows seasonal and spatial variety [5, 6]. Although effective measures have been adopted to control SO_2 emissions since 1990 [7, 8], energy demand and the energy structure make SO_2 pollution an attention-worthy problem in China.

Increasing research shows that the reactions of trace gases with particles play an important role in atmospheric chemistry. The heterogeneous reaction of SO_2 on particle surfaces is another pathway for SO_2 depletion and sulfate formation. Studies since the 1970s have demonstrated that the uptake of SO_2 on particles leads to sulfite and sulfate formation [9]. The reaction mechanism and kinetics are related to the physical and chemical characteristics of the particles, such as surface active sites, acidity, and surface area [10–13]. Studies have focused on mineral particles and sea salts. Goodman *et al.* [14] studied the reaction of SO_2 on α-Al_2O_3 and MgO, using a Knudsen cell and Fourier-transform infrared (FT-IR) spectroscopy. Ullerstam *et al*. [14] studied the reaction on mineral dust using DRIFTS and determined the uptake coefficient. A study of iron oxides showed the influence of surface hydrogen, oxygen, and surface adsorbed water [10, 16]. With the reaction on γ-Al_2O_3, the presence of NO_2 improved the oxidation of SO_2 [17]. Li *et al*. [11] studied the heterogeneous oxidation of SO_2 by ozone on the surface of sodium chloride and mixtures with other components using *in situ* DRIFTS and proposed a three-stage mechanism: (1) O_3 was adsorbed on the NaCl surface, which resulted in an alkalescent surface; (2) the adsorption of SO_2 was then followed by (3) O_3 oxidation. The adsorption of O_3 on the NaCl surface was the rate-determining

*Corresponding author (email: shangjing@pku.edu.cn; tzhu@pku.edu.cn)

step. The reaction was zero-order for SO_2 and first-order for O_3. The reaction uptake coefficients γ_{BET} and γ_{GEO} were determined to be about 10^{-8} and 10^{-5}, respectively. Li *et al*. [18, 19] also studied the reaction on $CaCO_3$ as representative mineral particles and proposed a two-step mechanism: (1) SO_2 was absorbed on wet $CaCO_3$ particles, leading to the formation of sulfite; and (2) the sulfite was quickly oxidized into sulfate by O_3. The adsorption of SO_2 was rate-determining and it could not happen on dry calcium carbonate. The reaction was first-order for SO_2 and zero-order for O_3 and γ_{BET} and γ_{GEO} were determined to be around 10^{-7} and 10^{-4}, respectively.

To date, most studies on the heterogeneous reaction of SO_2 on particles have examined dark environments and few have studied reactions with illumination. David *et al*. [20]. studied the SO_2 reaction on α-Fe_2O_3(0001) and found that UV illumination promoted the adsorption of SO_2. Tai *et al*. [21] showed that the consumption rate of SO_2 on α-Fe_2O_3 was faster in the presence of UV. Thus, the heterogeneous reaction of SO_2 on particles with illumination differs from that without illumination. Research examining the heterogeneous reaction of SO_2 with irradiation has practical importance. The n-type semi-conductor TiO_2 is excited by UV ($\lambda < 387$ nm) and produces photo-induced electrons and holes, resulting in active species that participate in atmospheric photochemical reactions, primarily O^{2-} and ·OH [22]. TiO_2 is used as a photocatalyst and an additive in paints, food, and make-up. Although it is far less abundant than other insulative oxides, like SiO_2, Al_2O_3, and MgO, the heterogeneous reaction on a TiO_2 surface is non-negligible and the heterogeneous photo-oxidative reaction is probably an important pathway for the transformation of air pollutants on particles. We use DRIFTS to study the heterogeneous reaction of SO_2 on TiO_2 particle surfaces. The influences of the oxygen concentration, relative humidity (RH), and UV light illumination ($\lambda \approx 365$ nm) intensity on the reaction were investigated. A mechanism for the heterogeneous reaction of SO_2 on TiO_2 particle surfaces was proposed.

2 Experiments

TiO_2 (Degussa, P-25) was used as purchased. The powder surface area was 49.89 m^2/g, measured using an ASAP2010 BET apparatus with multipoint Brunauer-Emmett-Teller (BET) analysis. The sample consisted of 70% anatase and 30% rutile, based on X-ray diffraction, and the particle diameter was about 20 nm, determined by transmission electron microscopy (H-9000NAR)

Infrared spectra were recorded in the spectral range from 4000 to 1000 cm^{-1} with a Nicolet Nexus FT-IR spectrometer equipped with a mercury cadmium telluride (MCT) detector and a DRIFTS optics accessory (model DRA-2CO, Harrick Scientific). Spectra were recorded at a resolution of 4 cm^{-1} and 128 scans were averaged for each spectrum with a time resolution of less than 2 min. The DRIFTS reactor used in this experiment has been described in detail elsewhere [11]. The spectra are presented in K-M scale, which gives a better linear relationship with concentration [23].

Before the experiment, SO_2 (Beijing Huayuan Gas Chemical) was diluted and mixed with carrier gas. The flux of high purity N_2, high purity O_2, water vapor and air was controlled by mass flow controllers (MFCs), according to the experimental conditions, and the total flow was 200 sccm. The diluting gas was air in most experiments, although pure O_2 and N_2 were mixed to obtain different O_2 concentrations. The reaction chamber was flushed with N_2 for 1 h, and then for another 0.5 h while the sample was kept at 25 °C. This treatment removed most of the loosely adsorbed water, although water remained in the particles. A background spectrum was recorded at the end of the N_2 flush, and then a mixture of SO_2 at known concentrations and RH in N_2 or air was introduced to the reaction chamber. A typical experiment lasted for 180 min.

The RH was controlled using a saturated water vapor generator and measured using a Rotronic Humidity sensor (NT2-D) at the outlet of the DRIFTS equipment. The UV light was obtained with a 500 W xenon light (CHF-XM35). After filtering with a 365 band pass filter, the UV light was introduced into the DRIFTS reaction cell via a UV optical fiber.

The amounts of sulfite and sulfate ions formed during the reaction were measured by ion chromatography using a Dionex ICS 2500 system equipped with a Dionex AS 14 analytical column and a conductivity detector. The reacted sample was sonicated for 20 min in 5 mL of Milli-Q water containing 1% formaldehyde to protect sulfite. A single scrubber system with 1.5 mM Na_2CO_3/1.0 mM $NaHCO_3$ was used.

For the experiments, 0.025%–3% (wt) titanium sulfate was mixed with NaCl (Alfa Aesar). The mixtures were ground adequately, and then their DRIFTS spectra were recorded to calculate the relationship between the integrated area and concentration.

3 Results and discussion

3.1 Reaction of SO_2 on TiO_2 particle surfaces

3.1.1 Reaction on dry particles without UV

The sample was flushed with N_2 for 0.5 h and the negative adsorption peaks of water stopped decreasing. The background spectra were recorded, and then 50 ppm SO_2 was introduced. DRIFTS spectra for 0–3 h are shown in Figure 1. The spectra at 1000–1300 cm^{-1} were relatively disorderly, due to background adsorption of TiO_2. This region revealed the adsorption of sulfate and indicated that sulfate production was low.

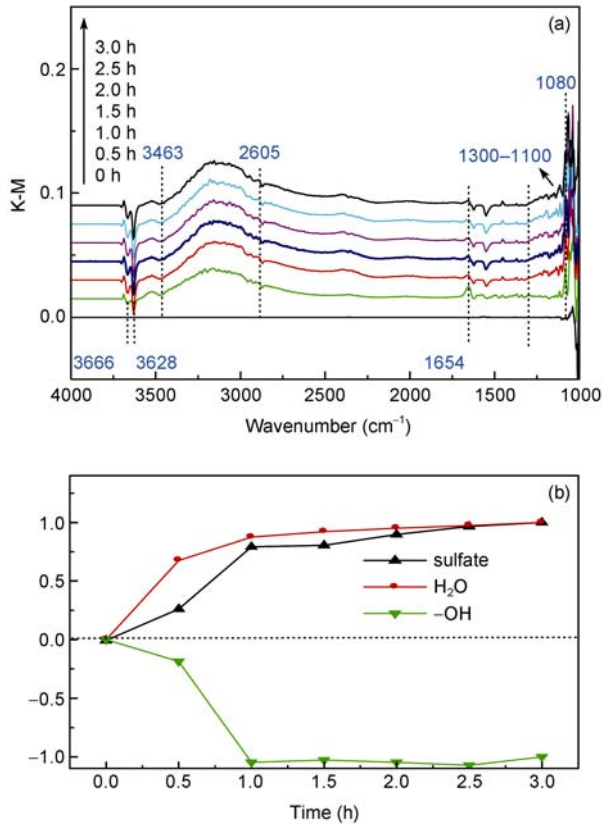

Figure 1 (a) DRIFTS spectra of the reaction of SO_2 on dry TiO_2 particles (C_{SO_2} = 50 ppm, air-diluted, without illumination). (b) Relationship of the integrated areas of sulfate (1300–1100 cm^{-1}), absorbed water (3218–3096 cm^{-1}), and hydroxyl (3666 cm^{-1}) with time in Figure 1(a); the data were normalized using the absolute value at 3 h.

As shown in Figure 1(a), after introducing SO_2, small, sharp, negative peaks appeared at 3666 and 3628 cm^{-1} and were attributed to the vibration of hydroxyl on Ti atoms. Obvious absorption at 3463–2605 cm^{-1}, centered on 3160 cm^{-1}, was observed and was assigned to surface water molecule adsorption, and the peak at 1654 cm^{-1} resulted from the H–O–H bending vibration [24]. Adsorption in the 1300–1100 cm^{-1} region was assigned to sulfate adsorption [23, 24] and the positive peak at 1080 cm^{-1} was attributed to the adsorption of SO_3^{2-} or HSO_3^- [24, 25]. Spectra below 1100 cm^{-1} were not sufficient for quantitative analysis, because of the stronger adsorption of TiO_2 in this region. Thus, only sulfate adsorption was analyzed quantitatively.

The integrated areas of 1300–1100, 3218–3096, and 3666 cm^{-1}, corresponding to adsorption by sulfate, absorbed water, and hydroxyl, were calculated. The data were normalized using the absolute value of that reacted for 3 h and the trend is shown in Figure 1(b). With increasing time, sulfate and absorbed water increased gradually, while hydroxyl decreased, revealing that hydroxyl was consumed in the reaction. Simultaneously, some absorbed water was produced on the particle surfaces [13, 26].

3.1.2 Influencing factors

(1) Influence of RH The reaction was allowed to proceed in a system with 50 ppm SO_2 (diluted with air and no illumination) and RH ranging from 0 to 90%. When water was present, adsorption due to liquid water appeared at 1800–3600 cm^{-1} and 1640 cm^{-1} (DRIFTS spectra not shown) and these bands were observed at 5 min when the RH was 20%. Surface hydroxyl adsorption occurred. The adsorption of sulfur-containing species below 1300 cm^{-1} was similar to that in Figure 1(a), although there was a slight shift, caused by vibration of the sulfate combination state [27]. The absorption intensity in the 1300–1100 cm^{-1} region was stronger than that on dry particles. Figure 2 illustrates the sulfate production at different RH for 2 h. Water obviously improved the production of sulfate, in proportion to the RH. Water molecules not only participated in the reaction as a reactant, they may also form a water film that benefited product diffusion and surface refreshment [1]. When the RH exceeded 80%, the total sulfate production was reduced. Excessive water may combine with the active sites on the particle surface and hinder the adsorption of SO_2 and further reaction.

(2) Influence of O_2 concentration The reaction proceeded

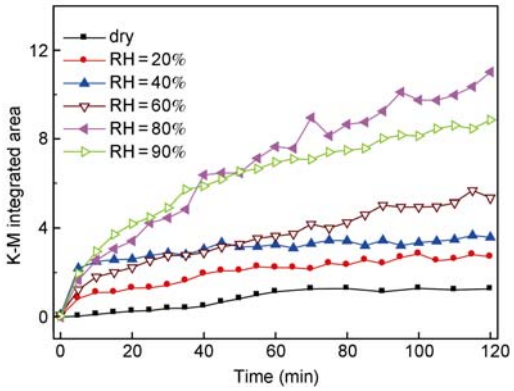

Figure 2 Sulfate production for various RH at 2 h (C_{SO_2} = 50 ppm, air-diluted, without illumination): integrated area at 1300–1100 cm^{-1}.

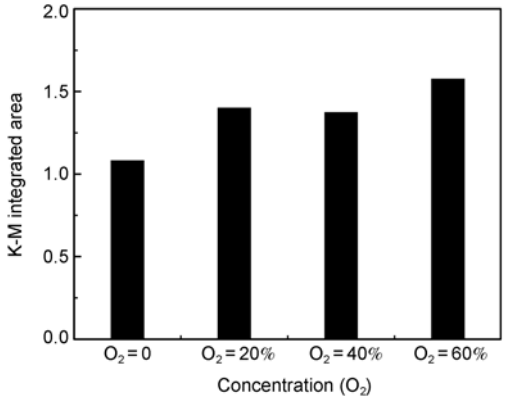

Figure 3 K-M integrated area of sulfate adsorption at 3 h for different O_2 concentrations (C_{SO_2} = 50 ppm, dry, without illumination): integrated area at 1300–1100 cm^{-1}.

at O_2 concentrations ranging from 0 to 60% (*v*/*v*) with 50 ppm SO_2 on dry particles. Figure 3 shows the K-M integrated area of sulfate adsorption at 3 h for different O_2 concentrations. As shown in Figure 3, sulfate production was enhanced slightly at greater O_2 concentrations. Generally, lattice oxygen and residual absorbed oxygen exist on particles surfaces. Meanwhile, trace amount of O_2 will be introduced into the reaction system by the high purity N_2. They could participate in the reaction [14, 28] and satisfy the oxygen demand.

(3) Influence of UV illumination The reaction of 50 ppm SO_2 with UV light illumination (365 nm, intensity = 24 μW/cm^2) was studied with dry gas mixtures and RH = 40%. DRIFTS spectra are shown in Figure 4(a) and (b). As seen in Figure 4(a), on dry particles peaks, sulfate adsorption was increased at 1144 and 1196 cm^{-1} in the 1300–1100 cm^{-1} region. When the RH was set at 40% (Figure 4(b)), sulfate production was enhanced significantly after subtracting the background increase. The adsorption band at 1170 cm^{-1} gradually became dominant.

The improvement in the reaction with UV illumination was related to the UV intensity. Experiments with different UV light intensities were conducted using dry particles and with the RH set at 40%. The corresponding kinetic curve for the sulfate production rate in 120 min is shown in Figures 4(c) and (d). This shows that the sulfate production at RH = 40% was greater than with dry particles. The sulfate production increased with the UV intensity, until saturation occurred at 285 μW/cm^2 on dry particles.

After reacting for 3 h, the greatest sulfate production was obtained in the system with the strongest UV intensity and RH = 40% (Figure 4(e)).

The K-M integrated area of sulfate (1300–1100 cm^{-1}) at 3 h was calculated for four systems: dry, without UV (dry); RH = 40%, without UV (RH = 40%); dry, with UV (UV); and RH = 40%, with UV (RH = 40% & UV). Water or UV illumination alone increased sulfate production (Figure 4(e)); UV had a stronger effect than water. The influence of UV was significantly improved in the presence of water and the sulfate production was greater than with water or UV illumination separately and even their summation, revealing a synergistic effect of the two. Figure 4(e) shows the increase (in percent) due to the synergistic effect.

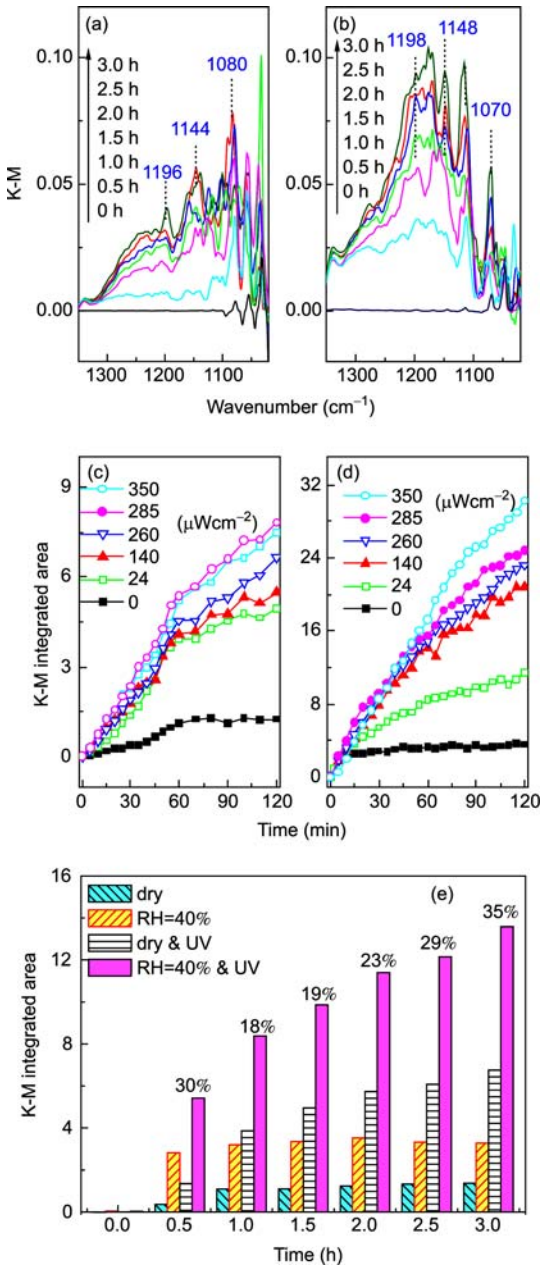

Figure 4 (a), (b) DRIFTS spectra of the SO_2 reaction on TiO_2 particles: (a) dry, (b) RH = 40% (C_{SO_2} = 50 ppm; air-diluted, 365 nm, intensity = 24 μW/cm^2, 1350–1020 cm^{-1} region). (c), (d) Sulfate production in 2 h at various UV intensities, (c) dry, (d) RH = 40% (C_{SO_2} = 50 ppm, air-diluted, 365 nm, 1300–1100 cm^{-1} region). (e) Sulfate production in 3 h for the four different systems (C_{SO_2} = 50 ppm, air-diluted, 1300–1100 cm^{-1} region).

3.2 Determination of reaction order and uptake coefficient

3.2.1 Kinetic curve of the SO_2 reaction

The reaction of various SO_2 concentrations was studied in two different systems: (a) dry, air diluted, no UV illumination; or (b) RH = 40%, air-diluted, with UV illumination at 365 nm and an intensity of 350 μW/cm^2. The kinetic curves of sulfate production are illustrated in Figure 5. In system (a), the kinetic curve had a turning point (Figure 5(a)), while in system (b), no obvious turning point was observed with SO_2 concentrations of 25 or 50 ppm (Figure 5(b)). Sulfate production kept increasing in both systems over 3 h. Both the sulfate production rate and amount were enhanced by higher SO_2 concentrations in an appropriate range. When the SO_2 concentration was increased to a certain point (400 ppm), the initial reaction rate and final amount of sulfate stopped increasing (Figure 5(a)). An excessive SO_2 concentration caused rapid sulfate production as most surface active

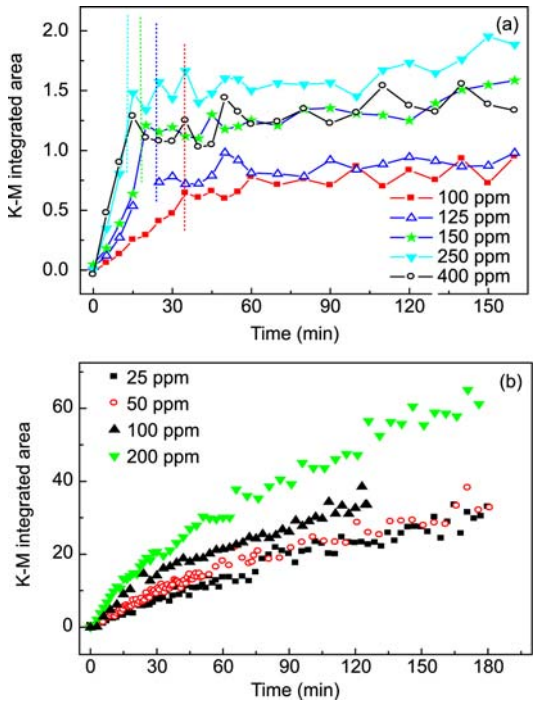

Figure 5 Kinetic curves of sulfate production at different SO_2 concentrations (1300–1100 cm^{-1} region): (a) dry, air-diluted, without UV illumination; (b) RH = 40%, air-diluted, with UV illumination at 350 μW/cm^2.

sites were occupied. Beyond this, the activity of particles was reduced [29, 30] and the reaction was hindered.

3.2.2 *Quantification of sulfate production*

After measured by DRIFTS, samples reacted under different condition or reacted for different time were instantly tested using IC. However, the amount of sulfite and sulfate detected by IC and DRIFTS showed no obviously relationship (figure omitted). Since IC method measures the average concentration of all the sample in a depth of 0.5 mm and the detecting depth of DRIFTS is probably several micrometers, it can be inferred that the production was not identical at different depths. The reaction without UV illumination resulted in sulfite primarily, while the dominant product in the presence of UV illumination was sulfate. This indicates that SO_2 molecules penetrated deeper than the UV illumination did. Consequently, it was not reasonable to regress the relationship of sulfate amount and the K-M integrated area using the bulk average concentration, determined by IC. We adopted a direct method, which calculated the relationship by measuring the K-M integrated area at 1300–1100 cm^{-1} of a fully ground mixture of NaCl with different ratios of $Ti(SO_4)_2$. The measurement conditions basically met the K-M quantitative demands. A linear relationship was obtained and the conversion factor was 1.05×10^{16} molecules per unit of K-M integrated area ($R^2 = 0.93$).

3.2.3 *Reaction order and uptake coefficient*

Because increasing SO_2 concentrations accelerated the reaction, the heterogeneous reaction of SO_2 on the TiO_2 particles was related to the SO_2 concentration and active sites on the particle surfaces. According to the law of mass action, the sulfate production rate can be expressed as:

$$\mathrm{d}\left[\mathrm{SO_4^{2-}}\right]/\mathrm{d}t = k\left[\mathrm{SO_2}\right]^m\left[\mathrm{TiO_2}\right]^n\left[\mathrm{H_2O}\right]^p \quad (1)$$

where $[SO_4^{2-}]$ is the sulfate concentration on TiO_2 particle surfaces, $[SO_2]$ is the SO_2 gas concentration, $[TiO_2]$ is the concentration of active sites on the TiO_2 particle surfaces, and $[H_2O]$ is the surface water concentration, and m, n, and p are the reaction orders of SO_2 gas, surface active sites, and surface water molecules, respectively.

Initially, the decrease in surface active sites was negligible compared with the total number of active sites. At this stage, the $[TiO_2]$ was approximately constant. In the reactions with different SO_2 concentrations and the same RH, taking the logarithm of formula (1) gives the following:

$$\ln\left(\mathrm{d}\left[\mathrm{SO_4^{2-}}\right]/\mathrm{d}t\right) = \ln k + m\ln\left[\mathrm{SO_2}\right] + n\ln\left[\mathrm{TiO_2}\right] + p\ln\left[\mathrm{H_2O}\right] \quad (2)$$

When the sulfate production increased with the SO_2 concentration, the sulfate production rate (ion/(s·g)) could be calculated from the kinetic curve. The sulfate production rates according to the SO_2 concentration for the [dry] and [RH = 40% & UV] systems are shown in Figures 6(a) and (b), respectively. In the [dry] system, the reaction order of the SO_2 concentration was 1.84, which is close to a second-order reaction. In the [RH = 40% & UV] system, the reaction order for the SO_2 concentration was 0.51, which approximates a first-order reaction.

The uptake coefficient is an important parameter in a heterogeneous reaction because it describes the reaction rate. In this study, the reaction uptake coefficient was defined as ratio of the number of sulfate ions produced to the number of SO_2 molecules colliding with particles [14]. When the

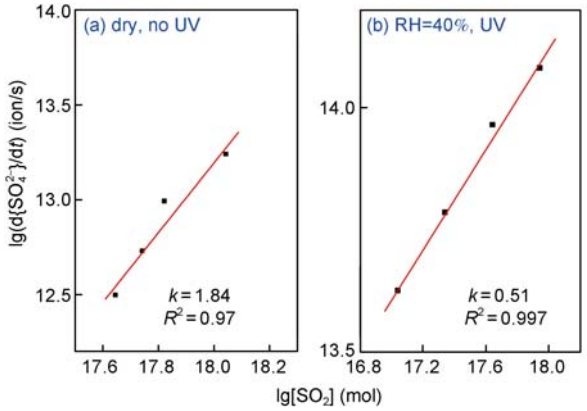

Figure 6 Log-log curve of the sulfate production rate plotted against the SO_2 concentration: (a) dry, without UV illumination, C_{SO_2} = 100–250 ppm; (b) RH = 40%; with 365 nm UV illumination at 350 μW/cm^2; C_{SO_2} = 25–200 ppm.

SO_2 concentration was 50 ppm, the initial reaction uptake coefficient using the BET surface as the reacting surface, $\gamma_{BET,}$ was determined to be 1.94×10^{-6} and 1.35×10^{-5} for the [dry] and [RH = 40% & UV] systems, respectively. The uptake coefficient in the system with UV illumination and some water was about 6 times greater than for the dry system.

3.3 Discussion of the reaction mechanism

3.3.1 Dry system without UV illumination

In the dry system without UV illumination, SO_2 reacted with TiO_2 particles, forming sulfite and sulfate. Surface hydroxyl was consumed, while some water was produced in the reaction. The deduced mechanism was as follows: gaseous SO_2 molecules were adsorbed on the TiO_2 particles becoming SO_{2ads} ("ads" indicates adsorbed); the SO_{2ads} reacted with surface hydroxyl and adsorbed oxygen [10, 25] to produce SO_3^{2-} and HSO_3^-; the product was further oxidized into SO_4^{2-} and HSO_4^-, as indicated by formulaes (3) to (6):

$$SO_{2ads}+OH^-\rightarrow HSO_3^- \quad (3)$$

$$SO_{2ads}+2OH^-\rightarrow SO_3^{2-}+H_2O \quad (4)$$

$$O_2+[M]\rightarrow O-[M] \quad (5)$$

$$SO_3^{2-}\left(\text{or}HSO_3^-\right)+O\text{–}\left[M\right]\rightarrow SO_4^{2-}\left(\text{or }HSO_4^-\right) \quad (6)$$

3.3.2 System with UV illumination and a set RH

SO_2 is excited by 365 nm UV light, producing $^3SO_2$, which reacts homogeneously with SO_2 and O_2 and produces gaseous SO_3, which is transformed into sulfate acid in the presence of water. On photocatalytic particles, SO_3 produced via the homogeneous reaction constituted 3.2% of that produced by heterogeneous photo-oxidation [30]. Here, we focused on the mechanism of sulfate production via heterogeneous photo-oxidation.

When the RH was 20%, liquid water formed on the particle surface and the reaction was close to a liquid reaction. SO_{2ads} reacted with water molecules and HSO_3^- and SO_3^{2-} [2, 14] were formed, as shown in formulaes (7) and (8):

$$SO_{2ads}+H_2O\leftrightarrow SO_2\cdot H_2O\leftrightarrow H^++HSO_3^- \quad (7)$$

$$HSO_3^-\leftrightarrow H^++SO_3^{2-} \quad (8)$$

With UV illumination in the presence of water (*i.e.*, RH > 10), the reaction of SO_2 on TiO_2 particles was enhanced. TiO_2 is an n-type semiconductor and with 365 nm irradiation it generates photo-induced electrons (e_{cb}^-) and holes (h_{vb}^+) on the conduction band (CB) and valence band (VB), respectively. e_{cb}^- and h_{vb}^+ are very active and they will react with surface oxygen and water (or OH^-) and produce O_2^- and ·OH [31].

As Figure 4(e) shows, the sulfate production in the [RH = 40%] system reached saturation at about 2 h. For the [RH = 40% & UV] system, water accelerated sulfate production for 3 h. The ·OH generated on UV illumination played an important role. Comparing sulfate production in the [dry] and [dry & UV] systems, the role of UV illumination in the [dry & UV] system was attributed to O_2^-, although a role of ·OH cannot be excluded. In Figures 4(c) and (d), the [dry & UV] and [RH = 40% & UV] systems were compared and this showed that the UV illuminated reaction increased sulfate formation in the presence of RH. O_2 was present in both systems. Based on the above analysis, we believe that active oxygen species were important in the systems with UV illumination. These attack O_2 molecules and the oxidation of SO_2 and sulfate formation were both improved significantly. ·OH had a greater role than O_2^- species. The proposed mechanism was as follows:

$$SO_{2ads}+\cdot HO\rightarrow HOSO_2 \quad (9)$$

$$HOSO_2+O_{2ads}\rightarrow HO_2+SO_3 \quad (10)$$

$$SO_{2ads}+O_2^-\rightarrow SO_3+O^- \quad (11)$$

$$SO_3+H_2O\rightarrow H_2SO_4 \quad (12)$$

4 Conclusions

The heterogeneous reaction of SO_2 occurred on TiO_2 particles and sulfite and sulfate were produced. Both UV illumination and water enhanced the reaction and they had a synergistic effect. Active oxygen species generated on irradiated TiO_2 particles played an important role in the reaction.

In the [dry & no UV] system, the heterogeneous reaction of SO_2 on TiO_2 particles was found to be second-order for SO_2 and the initial uptake coefficient, γ_{BET}, was determined to be 1.94×10^{-6}. With UV and RH = 40%, the reaction order was first-order and the initial uptake coefficient was 1.35×10^{-5}. Atmospheric chemistry reactions always happen at RH > 0 and the uptake of SO_2 on semiconductor TiO_2 is increased significantly during the day. Thus, heterogeneous reactions on photocatalytic particles may be important.

This work was supported by the National Basic Research Program of China (2002CB410802), National Natural Science Fundation of China (20407002), and special fund of State Key Joint Laboratory of Environment Simulation and Pollution Control.

1 Tang XY, Zhang YH, Shao M. *Atmospheric Environmental Chemistry* (in Chinese). Beijing: Higher Education Press, 2006
2 Dai SG. *Environmental Chemistry* (in Chinese). Beijing: Higher Education Press, 2006
3 Zhang Q, Stanier CO, Canagaratna MR. Insights into the chemistry

of new particle formation and growth events in Pittsburgh based on aerosol mass spectrometry. *Environ Sci Tech*, 2004, 38: 4797–4809
4 Sunyer J, Atkinson R, Ballester F. Respiratory effects of sulphur dioxide: A hierarchical multicity analysis in the APHEA2 study. *Occup Environ Med,* 60(8): e2
5 Arndt RL, Carmichael GR, Streets DG. Sulfur dioxide emissions and sectorial contributions to sulfur deposition in Asia. *Atmos Environ*, 1997, 31(10): 1553–1572
6 Wang D X, Deng W. Atmospheric SO_2 pollution and acidity of rain in changchun China. *Water Air Soil Pollution*, 2001, 130: 1631–1634
7 Gao CL, Yin HQ, Ai NS. Historical analysis of SO_2 pollution control policies in China. *Environ Manag*, 2009, 43: 447–457
8 Chan CK, Yao XH. Air pollution in mega cities in China. *Atmos Environ*, 2008, 42: 1–42
9 Usher CR, Michel A, Grassian VH. Reaction on mineral dust. *Chem Rev*, 2003, 103: 4883–4939
10 Fu H, Wang X, Wu H. Heterogeneous uptake and oxidation of SO_2 on iron oxides. *J Phys Chem C*, 2007, 111(16): 6077–6085
11 Li L, Chen ZM, Zhang YH. Heterogeneous oxidation of sulfur dioxide by ozone on the surface of sodium chloride and its mixtures with other components. *J Geophys Res*, 2007,112: D18301
12 Zhang XY, Zhuang GS, Chen JM. Heterogeneous reactions of sulfur dioxide on typical mineral particles. *J Phys Chem B*, 2006, 110(25): 12588–12596
13 Shang Y, Zhu T, Li Y, Zhao JC. Size-dependent hydroxyl radicals generation induced by SiO_2 ultra-fine particles: The role of surface iron. 2009, 52(7): 1033–1041
14 Goodman AL, Li P, Usher CR. Heterogeneous uptake of sulfur dioxide on aluminum and magnesium oxide particles. *J Phys Chem A*, 2001, 105(25): 6109–6120
15 Ullerstam M, Vogt R, Langer S, Ljungstrom E. The kinetics and mechanism of SO_2 oxidation by O_3 on mineral dust. *Phys Chem Chem Phys*, 2002, 4: 4604–4699
16 Zhang QJ, Wang X, Chen JM. Formation of Fe(II) (aq) and sulfate via heterogeneous reaction of $SO_2$with Fe_2O_3 (in Chinese). *Chem J Chinese Univ*, 2006, 27(7): 1347–1350
17 Ma QX, Liu YC, He H. Synergistic effect between NO_2 and SO_2 in their adsorption and reaction on γ-Alumina. *J Phys Chem A*, 2008, 112: 6630–6635
18 Li L, Chen Z M, Ding J. A DRIFTS study of SO_2 oxidation on the surface of $CaCO_3$ particles. *Spectros Spectral Anal*, 2004, 24(12), 1556–1559
19 Li L, Chen ZM, Zhang YH. Kinetics and mechanism of heterogeneous oxidation of sulfur dioxide by ozone on surface of calcium carbonate. *Atmos Chem Phys Disc*, 2006, 6, 2453–2464
20 David ST, Victor EH. Kinetics of SO_2 adsorption on photoexcited γ-Fe_2O_3. *J Phys Chem B*, 2001, 105(18): 3872–3877
21 Tai JJ, Fu HB, Kong LD. A mechanism observation on the photochemical reaction between SO_2 and α-Fe_2O_3 (in Chinese). *China Environ Sci*, 2008, 28(5): 401–406
22 Zakharenko V. Photoinduced heterogeneous processes on chemical phase components of solid tropospheric aerosols. *Top Catal*, 2005, 35(3-4): 231–236
23 Weng SF. *Fourier Transform Infrared spectroScopy Meter* (in Chinese). Beijing: Chemical Industry Press, 2005
24 Nakamoto K. *Infrared and Raman spectra of inorganic and Coordination Compounds*. 5th ed. New York: Wiley, 1997
25 Davydov A. *Molecular Spectroscopy of Oxide Catalyst Surface*. New York: Wiely, 2003
26 Gao YC, Chen D. Heterogeneous reactions of sulfur dioxide on dust. *Sci China: Ser B Chem*, 2006, 49(3): 273–280
27 Hiroyuki K, Hiroaki O, Katsumi T. SO_2 oxidation over the V_2O_5/TiO_2 SCR catalyst. *Catal Lett*, 2001, 73(1): 79–83
28 Sayago DI, Serrano P, Bohme O. A photoemission study of the SO_2 adsorption on TiO_2 (1100) surfaces. *Surf Sci*, 2001, 482-485: 9–14
29 Kim MR, Woo SI. Poisoning effect of SO_2 on the catalytic activity of Au/TiO_2 investigated with XPS and *in situ* FT-IR. *Appl Cata A-Gene*, 2006, 299: 52–57
30 Shang J, Zhu YF, Du YG. Comparative studies on the deactivation and regeneration of TiO_2 nanoparticles in three photocatalytic oxidation systems: C_7H_{16}, SO_2, and C_7H_{16}-SO_2. *J Solid State Chem*, 2002, 166(2): 395–399
31 Hoffmann MR, Martin ST, Choi WY. Environmental applications of semiconductor photocatalysis. *Chem Rev*, 1995, 95(1): 69–96